Bioactive Materials 5 (2020) 880–890

Contents lists available at ScienceDirect

Bioactive Materials

journal homepage: http://www.keaipublishing.com/biomat

Substrate stiffness modulates bone marrow-derived macrophage polarization through NF-κB signaling pathway

Mimi Chen[a,1], Yu Zhang[a,1], Pinghui Zhou[a], Xingzhi Liu[a], Huan Zhao[a], Xichao Zhou[a], Qiaoli Gu[a], Bin Li[a,**], Xuesong Zhu[a,***], Qin Shi[a,b,*]

[a] Department of Orthopedics, The First Affiliated Hospital of Soochow University, Orthopedic Institute, Medical College, Soochow University, 188 Shizi Road, Suzhou, Jiangsu, 215006, PR China
[b] Key Laboratory of Stem Cells and Biomedical Materials of Jiangsu Province and Chinese Ministry of Science and Technology, 199 Renai Road, Suzhou, 215123, PR China

ARTICLE INFO

Keywords:
Substrate stiffness
Macrophage polarization
NF-κB signaling pathway

ABSTRACT

The stiffness of the extracellular matrix (ECM) plays an important role in regulating the cellular programming. However, the mechanical characteristics of ECM affecting cell differentiation are still under investigated. Herein, we aimed to study the effect of ECM substrate stiffness on macrophage polarization. We prepared polyacrylamide hydrogels with different substrate stiffness, respectively. After the hydrogels were confirmed to have a good biocompatibility, the bone marrow-derived macrophages (BMMs) from mice were incubated on the hydrogels. With simulated by the low substrate stiffness, BMMs displayed an enhanced expression of CD86 on the cell surface and production of reactive oxygen species (ROS) in cells, and secreted more IL-1β and TNF-α in the supernatant. On the contrary, stressed by the medium stiffness, BMMs expressed more CD206, produced less ROS, and secreted more IL-4 and TGF-β. In vivo study by delivered the hydrogels subcutaneously in mice, more $CD68^+CD86^+$ cells around the hydrogels with the low substrate stiffness were observed while more $CD68^+CD206^+$ cells near by the middle stiffness hydrogels. In addition, the expressions of NIK, phosphorylated p65 (pi-p65) and phosphorylated IκB (pi-IκB) were significantly increased after stimulation with low stiffness in BMMs. Taken together, these findings demonstrated that substrate stiffness could affect macrophages polarization. Low substrate stiffness promoted BMMs to shift to classically activated macrophages (M1) and the middle one to alternatively activated macrophages (M2), through modulating ROS-initiated NF-κB pathway. Therefore, we anticipated ECM-based substrate stiffness with immune modulation would be under consideration in the clinical applications if necessary.

1. Introduction

The extracellular matrices (ECMs) are involved in various cellular processes, such as proliferation, differentiation, survival and morphogenesis. ECMs not only provide physical support, but also offer favorable micro-environment to cells [1–3]. Extracellular stimulations, including soluble and adhesive factors, primarily bind to cell surface receptors and interact with cells, consequence regulate cell physiological activities. Moreover, mechanical properties of the ECMs, particularly rigidity or stiffness, can mediate cell signal and regulate the physiological processes, such as angiogenesis, organogenesis, immune response, and wound healing [4,5]. As an indicative parameter of ECMs, substrate stiffness can influence the stem cell fate in either 2-dimension or 3-dimension culture system [6]. By the integrin activation and internalization, the soft substrates can mimic the soft brain tissues to promote the neurogenic differentiation derived from mesenchymal stem cells (MSCs) [7]. On the contrary, the comparatively rigid matrices can mimic collagenous bone to accelerate osteogenic differentiation [8]. Pathologically, ECM remodeling and stiffening are accompanied with tumor progression by stimulating the proliferation, survival, and migration of tumor cells [9]. Therefore, ECM stiffness influences the extracellular mechanical environment, further regulate physiological

Peer review under responsibility of KeAi Communications Co., Ltd.
* Corresponding author. Department of Orthopedics, the First Affiliated Hospital of Soochow University, Orthopedic Institute, Medical College, Soochow University, 188 Shizi Road, Suzhou, Jiangsu, 215006, PR China.
** Corresponding author.
*** Corresponding author.
E-mail addresses: binli@suda.edu.cn (B. Li), zhuxs@126.com (X. Zhu), shiqin@suda.edu.cn (Q. Shi).
[1] These authors contributed equally to this work.

https://doi.org/10.1016/j.bioactmat.2020.05.004
Received 17 March 2020; Received in revised form 6 May 2020; Accepted 23 May 2020

Table 1
The formula of the polyacrylamide hydrogels for different substrate stiffness.

Substrate stiffness	40% acrylamide solution (mL)	2% bis-acrylamide solution (mL)	DI Water (mL)	APS (μL)	TEMED (μL)
Low	1	0.75	8.25	100	10
Middle	2.5	1.5	6	100	10
High	2.5	4.5	3	100	10

and pathological cellular processes of all kinds of cells residents in the tissues or mobilized in the fluid. Several pathways have been reported to be relevant to these processes, a significant promotion of Wingless/Integrase (Wnt/β-catenin) pathway was observed in the cells in the presence of the stiff ECMs [10]. It is well documented macrophages and stem cells have identified different signaling pathway that are initiated by this ECM stiffness, including Wnt/β-catenin, mitogen-activated protein kinases (MAPKs) and so on [11–13].

Macrophages are a highly heterogeneous population that derived from the myeloid cell lineages [14,15]. The common myeloid progenitor cell within the bone marrow are developed into mature monocytes by stimulating with the cytokines granulocyte-macrophage colony stimulating factor (GM-CSF) and macrophage colony stimulating factor (M-CSF), the cells enter the bloodstream and reside for several days before moving to tissues to become residential macrophages [16,17]. As a part of the innate immune system, macrophages are relevant to defense against invading pathogens [18,19]. They also take part in the progression of pathophysiological conditions such as cancer, cardiovascular diseases, wound healing, and foreign body response (FBR) [20].Simply, macrophage activation is often categorized into two extremes: classically activated (M1) and alternatively activated (M2) [21,22]. In the early stage of inflammation, macrophages are activated and polarized to a M1 phenotype. In the presence of interferon-γ (IFN-γ) and bacterial endotoxin lipopolysaccharide (LPS), the pro-inflammatory M1 macrophages, could produce intracellular nitric oxide (NO), tumor necrosis factor-α (TNF-α), IL-12, and IL-23, which lead to the inflammatory response [23]. They are helpful for defending against infections. During the resolution of inflammation, macrophages are predominantly differentiated to an M2 phenotype which secretes IL-4 and IL-10 to suppress inflammation, clear the debris, and restore tissue homeostasis. In addition, M2 macrophages could produce growth factors, such as transforming growth factor (TGF-β) and vascular endothelial growth factor (VEGF), which promote angiogenesis and tissue regeneration. Substance-P (SP), a neuropeptide, can induce inflammatory macrophages migrated to the spinal cord injury site to polarize to M2 and improved functional recovery [24,25]. With the development of tissue engineering, more and more ECM-based biomaterials are applied in regeneration medicine [26].

Several physical factors of ECMs have been evidenced to influence macrophages polarization and determine the outcomes of wound healing and tissue remodeling, including stiffness, topography and so on [27–29]. In this context, the effects of substrate stiffness on macrophage polarization need to be extensively underlined in biomaterial science and is of great significance in clinical medicine. The polyacrylamide hydrogels have been used to mimic ECMs, due to its suitable mechanical strength, biocompatibility and adjustable physicochemical properties for cell culture [20]. In the present study, we designed the polyacrylamide scaffolds with variable substrate modulus to investigate the effects of the polymeric substrate stiffness on macrophage polarization as well as the molecular mechanisms involved.

2. Materials and methods

All the procedures related to animals were performed in accordance with the Guide for the Care and Use of Laboratory Animals from the National Institutes of Health and the protocol was approved by the Animal Care and Use Committee of Soochow University.

2.1. Bone marrow-derived macrophages (BMMs) isolation and culture

Macrophages were isolated from bone marrow of the 6-week-old female C57BL/6 mice. After the mice were euthanized, the femurs and tibias were collected. The bone marrow cavities were repeatedly flushed with culture medium (αMEM, Hyclone, USA) containing 10% fetal bovine serum (FBS, Gibco, USA). After red cells were removed, the remained cells were cultured for further 12–16h. Non-adherent cells were harvested and seeded in the complete culture medium containing 30 ng/mL M-CSF (R&D, USA) for 72h to obtain BMMs [30].

2.2. Preparation of the polyacrylamide hydrogels with different substrate stiffness

Acrylamide (40% w/v), N,N′-Methylenebisacrylamide (2% w/v), ammonium persulfate (APS, 10% w/v) and tetramethylethylenediamine (TEMED) were mixed with deionized (DI) water in proportion and the liquid was added into the gap of the double glass plate. After the hydrogels were formed completely, a circular gel piece was made using the corresponding punch. Different substrate stiffness of the polyacrylamide hydrogels was developed by modulating the concentration of cross-linker agents (Table 1), we referred to the substrate stiffness of the three hydrogels as low, medium and high. BMMs were plated on the polyacrylamide hydrogels. BMMs were plated on tissue culture plate (TCP) as the control group. Partial hydrogels were soaked in the culture medium for 48h to obtain the leachate.

2.3. Cell proliferation assay

Raw264.7 cells (murine mononuclear macrophage leukemia cells) were seeded in the 96-well plates with the polyacrylamide hydrogel leachate or on the hydrogels directly. At the end of the experiment, cell counting kit (CCK-8) solution (10μL/well, Dojindo Laboratories, Japan) was added to each well, and cells were incubated for another 2h. Cell viability was determined using a microplate reader (BioTek, Vermont, USA) to read the optical density (OD) at an absorbance of 450 nm.

2.4. Live/dead cell staining

Live/dead cell staining kit (Thermo fisher scientific, USA) was applied to explore the toxicity of the hydrogels to cells. In brief, BMMs (5×10^4 cells/well) were cultured in the leachate in the 96-well plates for 5d. Then, cells were incubated with fluorescent buffer for 0.5 h at room temperature according to the manufacturer's instruction. BMMs were washed twice with phosphate buffer saline (PBS) to remove the unbounding fluorescent reagents. The live (green) or dead (red) cells were observed and imaged by a fluorescence microscope (Zeiss AxioImager, Germany).

2.5. Scanning electron microscope (SEM)

In briefs, BMMs were cultured on the polyacrylamide hydrogels for 3d and 5d, respectively. BMMs were fixed with 4% paraformaldehyde (PFA) for 0.5h. The cells were dehydrated by gradient alcohol and dried at the critical point. The morphology of BMMs on hydrogels were observed by SEM (FEI Quanta 200, USA).

2.6. Cytoskeleton staining

BMMs were cultured on the polyacrylamide hydrogels, respectively. According to the phalloidin staining kit protocols (Abcam, USA), BMMs were fixed with 4% PFA, then incubated with rhodamine-conjugated phalloidin to stain F-actin for 0.5h in the dark. BMMs were stained with 4′,6-diamidino-2-phenylindole (DAPI) for 10min in the dark, and observed by the fluorescent microscope (Zeiss AxioImager, Germany).

2.7. Analysis of macrophage phenotype by flow cytometry assay (FCA)

Macrophage phenotypic markers, CD68 and CD86 for M1 and CD68 and CD206 for M2, were selected following the previous study [31,32]. BMMs were cultured on the polyacrylamide hydrogels in the 24-well plates (3×10^5 cells/well) for 3d and 5d, respectively. Thereafter, the cells were stained with the fluorescent-conjugated antibodies (isotype control antibody, CD68, CD86 or CD206, eBioscience, USA) for 30 min at 4 ˚C. The expression of CD68, CD86 and CD206 on BMMs were assayed by FCA apparatus (Merck Millipore, Germany) and analyzed by FlowJo (BD, USA).

2.8. Immunofluorescence of macrophage-associated proteins

BMMs were seeded on the polyacrylamide hydrogels at a density of 4×10^4 cells/well in the presence of M-CSF (30 ng/mL) for 3d. BMMs were fixed and stained with fluorescent-conjugated antibodies. The specific steps were as follows: BMMs were fixed with 4% PFA for 15 min at room temperature, permeabilized with 0.1% Triton X-100 for 15min and blocked with 3% BSA-PBS for 1h. BMMs were incubated with primary antibody for overnight at 4 ˚C, secondary fluorescent antibody for 1h and DAPI (Abcam, USA) for 15min in dark place at 37 ˚C. Immunofluorescence images were collected using fluorescence microscope (Zeiss AxioImager, Germany).

2.9. Quantitative real time PCR (qRT-PCR)

BMMs (3×10^5 cells/well) were plated on the polyacrylamide hydrogels for 3d and 5d in the 6-well-plates, respectively. Total RNA of the seeded cell was isolated using Trizol reagent (Beyotime, China) according to the manufacturer's protocols and the concentration of total RNA was determined by NanoDrop2000 (Thermo Fisher Scientific, USA). Message RNA was reverse transcription to cDNA with the reverse transcriptase kit (TaKaRa, Japan). qRT-PCR were performed (CFX96™ Real-Time system, Bio-Rad, USA). The sequences of the target genes were listed in Table 2. The gene expression levels were normalized to β-actin expression and analyzed according to the comparative Ct ($2^{-\Delta\Delta Ct}$) method.

Table 2
Primer sequences specific to BMMs for qRT-PCR.

Gene		Primer (5′-3′)
IL-1β	sence	AGTTGACGGACCCCAAAAGA
	antisence	GGACAGCCCAGGTCAAAGG
iNOS	sence	ATGCCCGATGGCACCATCAGA
	antisence	TCTCCAGGCCCATCCTCCTGC
Arg	sence	TCACCTGAGCTTTGATGTCG
	antisence	CTGAAAGGAGCCCTGTCTTG
TGF-β	sence	TGCGCTTGCAGAGATTAAAA
	antisence	CGTCAAAAGACAGCCACTCA
β-actin	sence	TCATTGACCTCAACTACATGGT
	antisence	CTAAGCAGTTGGTGGTGCAG

2.10. Enzyme linked immunosorbent assay (ELISA) for cytokine expressions

BMMs were incubated on the polyacrylamide hydrogels for 3d and 5d, respectively. The concentrations of cytokine profiles in the culture supernatant were measured by ELISA assay kit (R&D Systems, USA) according to the manufacturer's instructions and calibrated by standard curve.

2.11. Measurement of reactive oxygen species (ROS) production

BMMs (3×10^5 cells/well) were plated on the polyacrylamide hydrogels with different substrate stiffness for 3d and 5d in the 6-well-plate. Fluorescent probes-2′, 7′-Dichlorofluorescent yellow diacetate (DCFH-DA, Beyotime, China) were diluted with serum-free medium to a final concentration of 5 μmol/L. Appropriate volume of diluted DCFH-DA was added to the incubated cells for 0.5 h at room temperature in dark. The cells were washed. The intensity of fluorescence was measured by FCA apparatus (Guava® easyCyte, Germany) and observed by a fluorescence microscope at 488 nm (Zeiss AxioImager, Germany).

2.12. Western blot

BMMs were seeded on the polyacrylamide hydrogels in the 6-well plates at density of 1.5×10^6 cells/well for 24h. Protein was extracted with protein lysates (Beyotime, China), the concentrations were measured using the BCA Protein Assay Kit (Beyotime, China). Equal amounts of total protein from cell lysates were electrophoresed in polyacrylamide hydrogels and transferred to nitrocellulose (NC) membrane from the polyacrylamide hydrogels. The nitrocellulose membranes were incubated with primary antibody (anti-IκB, NIK, p65, pi-p65, pi-IκB, Abcam, USA; anti-actin, Beyotime, China) with slight shaking at 4 ˚C for overnight. The NC membranes were washed and incubated horseradish peroxidase-conjugated secondary antibodies (goat anti-rabbit IgG, goat anti-mouse IgG, Beyotime, China) for 1h at room temperature, signals were detected by chemiluminescence. Protein bands were showed and semi-quantified by Image Lab software (Bio-Rad, USA).

2.13. Implantation of the polyacrylamide hydrogels to the mice subcutaneously

C57BL/6 mice (6-week-old, male) were anesthetized with 1.5% pentobarbital sodium intraperitoneally and the polyacrylamide hydrogels with different substrate stiffness (diameter 5 mm, thickness 0.75 mm) were implanted in the mice subcutaneously. After 14d, the animals were euthanized, and the implanted samples with neighbor skin were collected. Harvested tissues were dehydrated in 20%, 30% sucrose solution, fixed in 4% PFA and embedded in Tissue-Tek OCT compound (Sakura, USA) in order. Frozen sections were performed hematoxylin-eosin (H&E) staining and immunofluorescence staining (Mouse anti-CD68, rabbit anti-CD86 and CD206, Abcam, USA). Images were visualized using fluorescence microscope (Zeiss AxioImager, Germany) and the fluorescent density was quantified by Bioquant osteo (BIOQUANT, USA).

2.14. Statistical analysis

All the data were processed with IBM SPSS Statistics 22 for Windows. The data were presented as the mean ± standard (SD) obtained from three or more experiments and statistical significance determined by Student's t-test and One-way analysis of variance (ANOVA). Statistic differences were considered significantly at $p < 0.05$.

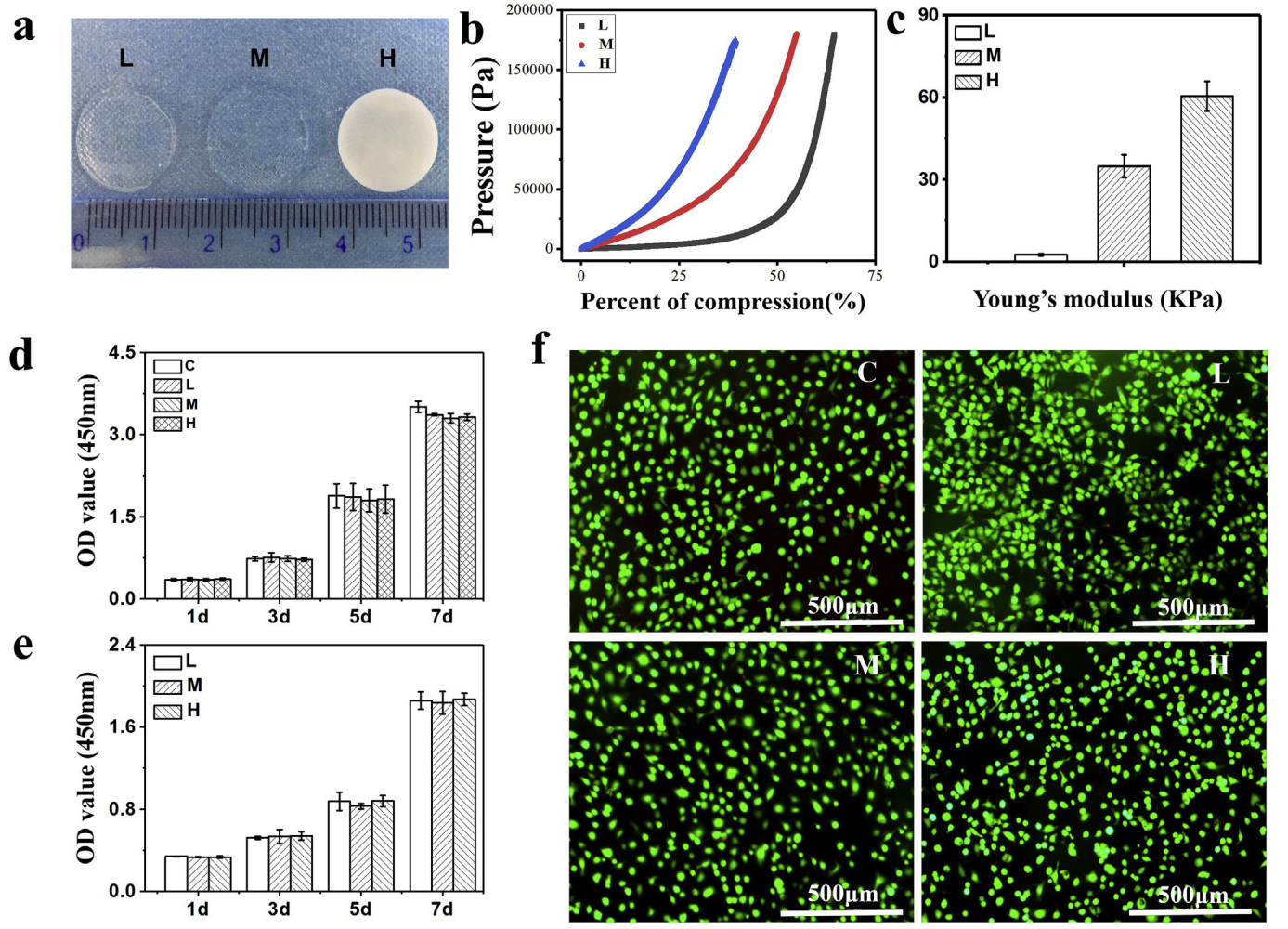

Fig. 1. Characterizations of the polyacrylamide hydrogels. (a) The images of the polyacrylamide hydrogels with different formula; (b) Compression test to measure the elastic modulus of polyacrylamide hydrogels with different formula, namely low (L), medium (M) and high (H) group according to its elastic modulus; (c) The Young's modulus of polyacrylamide hydrogels with different formula (n = 3); (d) The proliferation of Raw264.7 cells cultured in the leachate of polyacrylamide hydrogels (n = 5); (e) The proliferation of Raw264.7 cells seeded on the polyacrylamide hydrogels (n = 5); (f) The images of Raw264.7 cells cultured in the leachate for 5d stained by Live/dead cell staining kit. C: TCP, L: low substrate stiffness, M: middle substrate stiffness, H: high substrate stiffness.

3. Results

3.1. Polyacrylamide hydrogels have a good biocompatibility

The different elastic modulus polyacrylamide hydrogels are made by mixing with different proportions of acrylamide (40%) and dimethyi-bisacrylamide (2%). The morphology of the hydrogels with three kind of the substrate stiffness was displayed (Fig. 1a). With the concentrations of acrylamide and dimethyi-bisacrylamide increased, hydrogels became from transparent into non-transparent. Substrate stiffness of hydrogels was calculated from pressure and compression rate through the compression experiment (Fig. 1b). The substrate stiffness of polyacrylamide hydrogels was 2.55 ± 0.32 kPa, 34.88 ± 4.22 kPa and 63.53 ± 5.65 kPa (Fig. 1c), namely low, middle and high stiffness, respectively, which was comparable to the tissues of collagen fibers, osteoid and pre-calcified bone respectively [8,33,34].

Cell viability is one of the most important factors for evaluating biomedical scaffolds because it directly influences the final cellular activities, such as proliferation and differentiation. Therefore, we performed CCK-8 assay to check the viability of the cultured Raw264.7 cells. There was no significant growth difference between the experimental groups 1, 3, 5 and 7d after incubation, either cultured in the leachate or directly seeded on the materials (Fig. 1d–e). Raw264.7 cells proliferated well on the hydrogels with the different substrate stiffness, suggesting that polyacrylamide hydrogels were not harm to the cells.

Furthermore, cell status was confirmed by the live/dead cell staining 5d after culture. All the cells were similar morphologically, either in the presence of cell culture medium or the leachate of polyacrylamide hydrogels (Fig. 1f). In all, the developed polyacrylamide hydrogels displayed a good cytocompatibility, and the different substrate stiffness (within the certain range) did not affect cell proliferation [35–37].

3.2. Substrate stiffness affects the macrophage attachment and morphology

BMMs obtained from mice were seeded on the polyacrylamide hydrogels for 5d. Their cellular morphology and cell interaction were studied with SEM and F-actin staining. As Fig. 2a showed, cultured on the hydrogels with low and high stiffness for 3 and 5d, BMMs were presented in the shape of flat and round, pancake-like. The hydrogels with middle stiffness led BMMs to elongation, the cells became long and spindle-like. Fluorescence-labeled phalloidin can specifically bind to F-actin in eukaryotic cells, which displayed the distribution of the microfilament skeleton in the cells. As expected, F-actin immunofluorescence

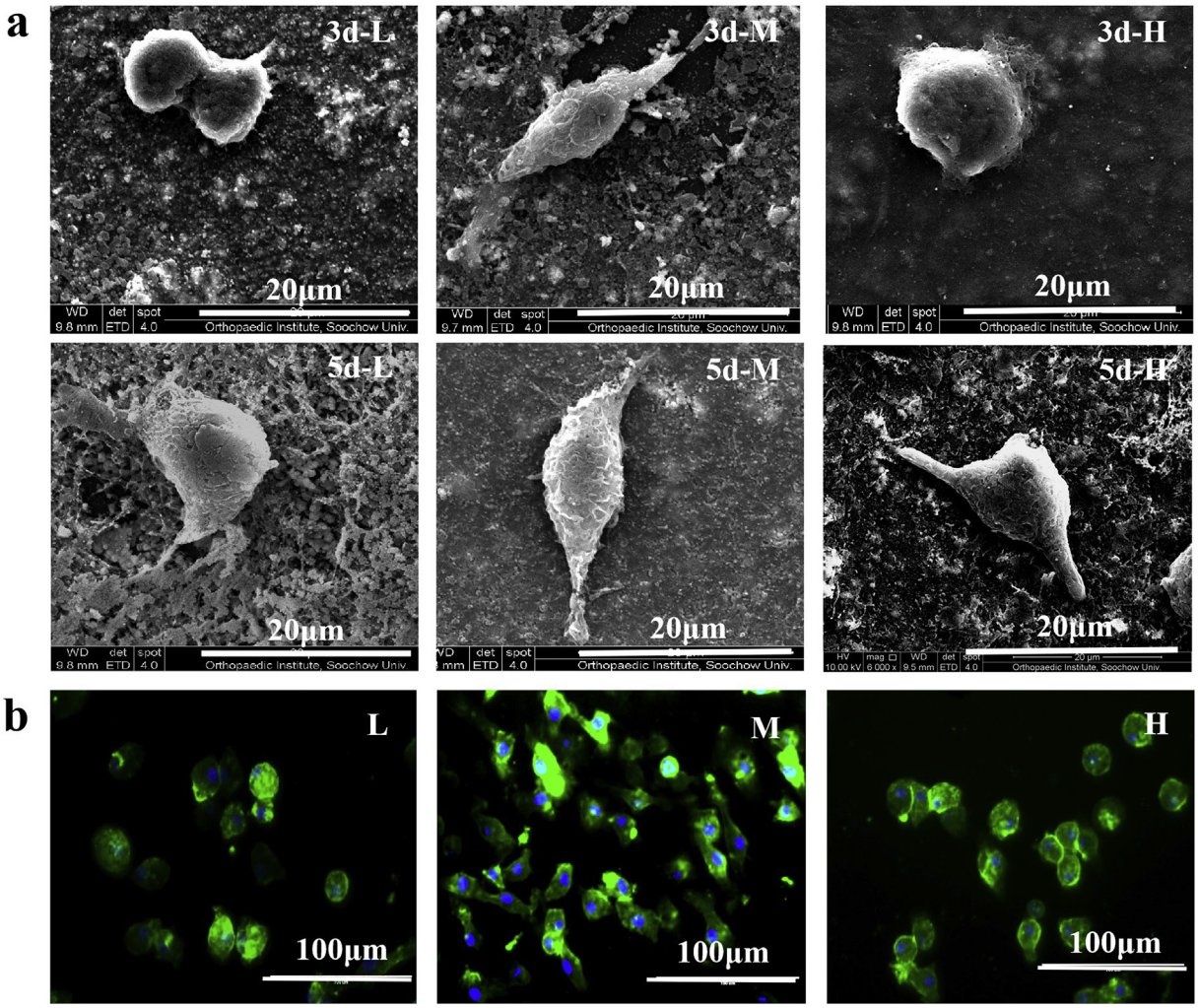

Fig. 2. The morphology and actin cytoskeleton of BMMs seeded on the polyacrylamide hydrogels with different stiffness. (a) The morphology of BMMs cultured for 3d and 5d, respectively, observed by SEM; (b) The F-actin cytoskeleton of BMMs cultured for 5d were observed by the fluorescent microscope with phalloidin-FITC (in green) and DAPI (in blue) staining. L: low substrate stiffness, M: middle substrate stiffness, H: high substrate stiffness.

staining further confirmed that the cells seeded on the middle substrate stiffness hydrogels for 5d looked flatter and more irregular than the cells seeded on the other hydrogels (Fig. 2b). Thus, different substrate stiffness affects the macrophage attachment and morphology. The hydrogel with a stiffness comparable to that of osteoid was more favorable for the cells to be adhesive and stretch, which may be one of the factors affecting the cell behaves.

3.3. Substrate stiffness changes the profiles of the surface protein expressed by the BMMs

It has been proved that M1 macrophages have an egg-shaped morphology, while M2 macrophages exhibited a more spindle-shaped morphology [31,38]. Since substrate stiffness affect cell morphology, we further analyzed the effect of substrate stiffness on the expression profiles of proteins produced by cells. BMMs seeded on polyacrylamide hydrogels for 3d and 5d, respectively, and the membrane protein expression was evaluated by FCA. The expression of CD86, a marker of M1 on CD68 positive cells displayed no significant difference between the three groups, neither 3d nor 5d. On the contrary, BMMs on the middle substrate stiffness hydrogels expressed significantly more CD206 (M2 marker) compared to the cells did on the low or high substrate stiffness hydrogels, either for 3d or 5d (Fig. 3a–d). To obtain a direct evidence on the polarization of BMMs, the expression of M1 and M2 related proteins of BMMs was examined by immunofluorescence staining on 3d and 5d (Fig. 3e–h). To our surprise, the CD86 fluorescence intensity of BMMs seeded with low stiffness was higher than the other two groups. More CD206 and less CD86 immunofluorescence staining was found on the cells with the middle and high substrate stiffness stimulation. It is indicative that middle substrate stiffness is beneficial for the macrophages to express CD206 molecules, suggesting an M2 shift exit. On the contrary, low substrate stiffness substrates may be favorable for M1 phenotype polarization.

3.4. Substrate stiffness modulates cytokine secretion by the BMMs

After the incubation for 3d and 5d, the cells and culture supernatants were collected separately and subjected to qRT-PCR and ELISA, respectively. As shown in Fig. 4a, the gene levels of IL-1β and iNOS expressed by BMMs treated with the low stiffness was about twice more than the ones by the cells treated with middle stiffness. Contrarily, the levels of anti-inflammatory genes were the lowest in the BMMs with low stiffness stimulation. BMMs seeded on the hydrogels with middle stiffness expressed TGF-β gene 1.25 times fold more than the cells with the low stiffness. Remarkably, Arg-1 gene expression of the BMMs with the middle stiffness was 4 times as expression as the one with low stiffness for 5d.

As for the cytokine's secretion, the general trend was corresponding

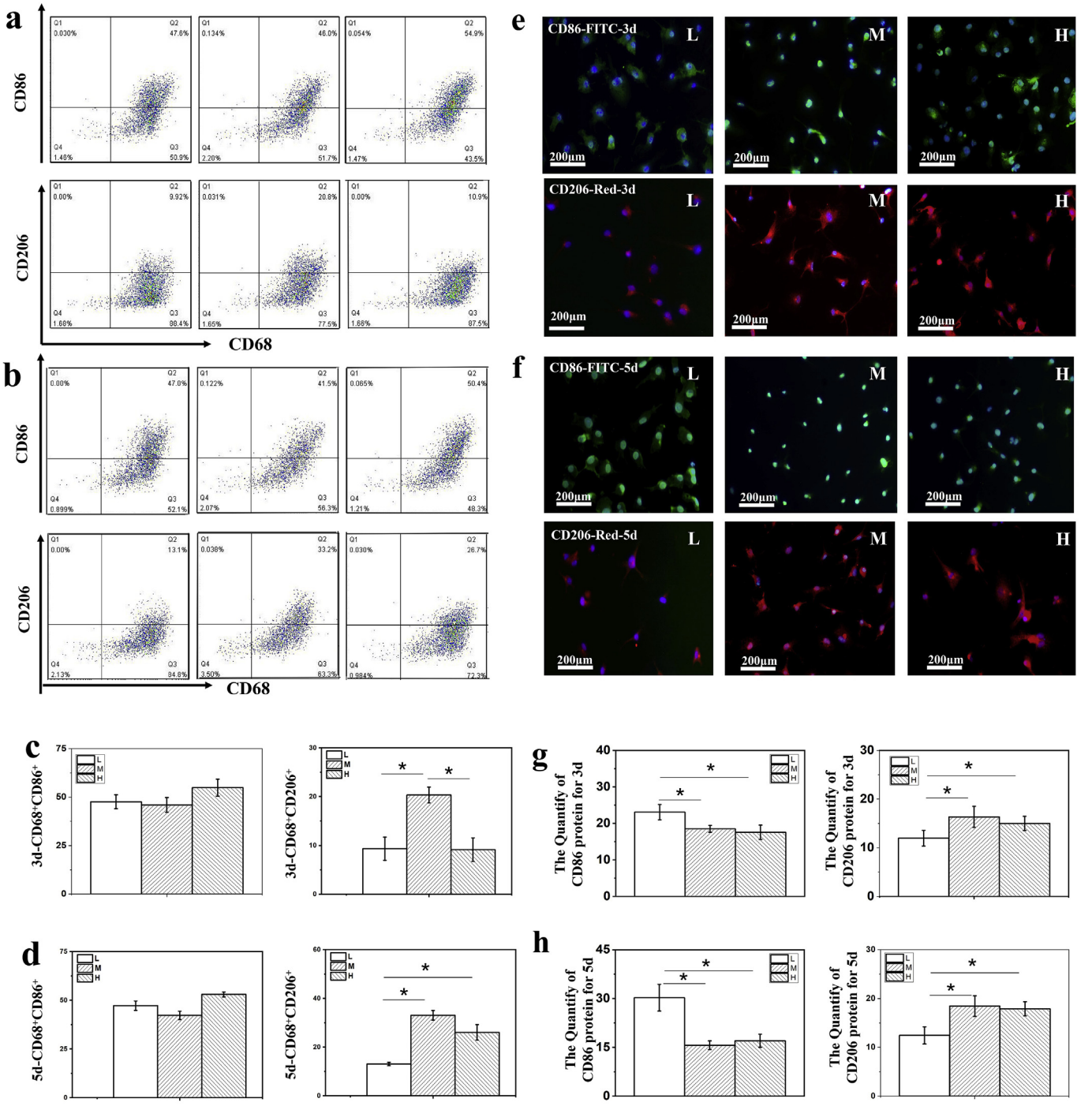

Fig. 3. Substrate stiffness monitored CD86 and CD206 expression of BMMs. BMMs were cultured on the polyacrylamide hydrogels with different stiffness. (a) and (b) the representative analysis of the expression of $CD68^+CD86^+$ and $CD68^+CD206^+$ BMMs by FCA for 3d and 5d, respectively; (c) and (d) the quantitative analysis of $CD68^+CD86^+$ and $CD68^+CD206^+$ BMMs for 3d and 5d, respectively; (e) (f) The expression of CD86 and CD206 of BMMs for 3d and 5d by immunofluorescence staining; (g) (h) Quantifying $CD86^+$ and $CD206^+$ immunofluorescence density by Image J for 3d and 5d (Rawak Software, Germany). L: low substrate stiffness, M: middle substrate stiffness, H: high substrate stiffness, n = 3, $^*p < 0.05$.

to gene expression (Fig. 4b). With the increase of substrate stiffness, the expression of IL-1β of the BMMs became fewer and fewer, while the expression of anti-inflammatory cytokines (IL-4, TGF-β) became more and more, either for 3d or 5d after incubation. Compared to the BMMs with low substrate stiffness stimulation, BMMs with middle or high modulus stimulation produced more pro-inflammation cytokine IL-1β and less anti-inflammation cytokines IL-4 and TGF-β. Thus, consisting to the previous FCA data, the data from gene and protein assays have further proven that substrate stiffness affect macrophage physiological process and the low substrate stiffness hydrogels polarize macrophages toward the classical phenotype.

3.5. Substrate stiffness influences the production of the reactive oxygen species (ROS) of BMMs

BMMs were incubated on the hydrogels with different substrate stiffness for 3d and 5d, respectively. BMMs incubated on low substrate stiffness hydrogels exhibited stronger green fluorescence than the cells

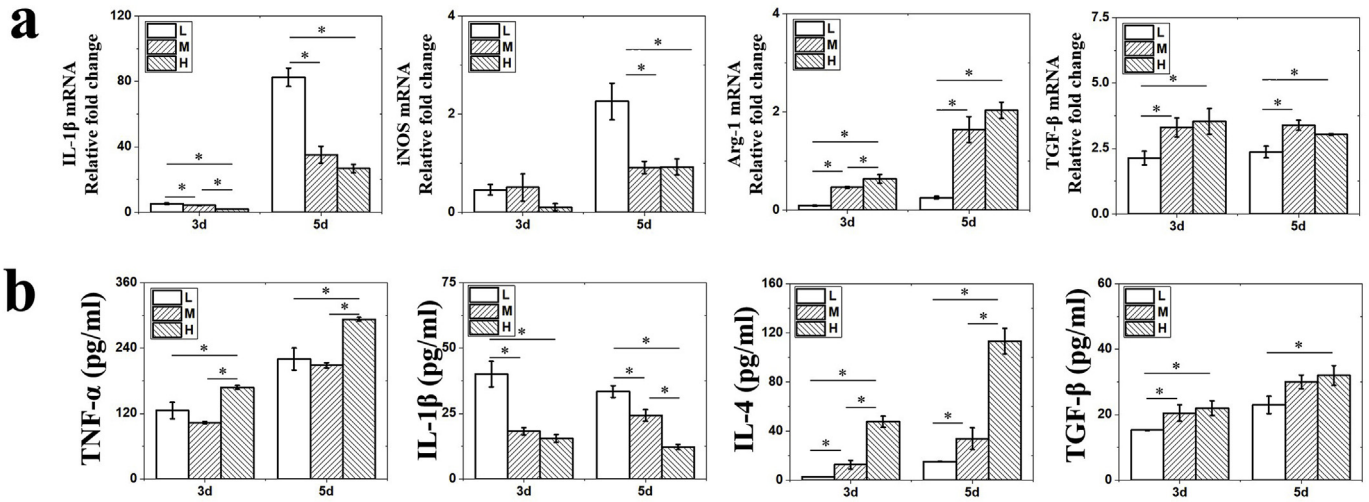

Fig. 4. Substrate stiffness regulated genes and cytokines expressions of BMMs. BMMs were cultured on the polyacrylamide hydrogels with different stiffness for 3 and 5d, respectively. (a) Gene expressions levels were normalized to β-actin of BMMs by qRT-PCR; (b) Secretion of cytokines in the supernatant of BMMs by ELISA. L: low substrate stiffness, M: middle substrate stiffness, H: high substrate stiffness, n = 3, *$p < 0.05$.

of the other two groups (Fig. 5a). Furthermore, the quantitative date of ROS production in BMMs by FAC demonstrated that the average fluorescence intensity of ROS decreased gradually with the substrate stiffness increased statistically (Fig. 5b). Moreover, in the same group, the productions of ROS of BMMs on 3d were more than the ones on 5d. Activated macrophages can produce large amounts of ROS. ROS production are higher in M1 macrophages compared to in M2 macrophages [39].

3.6. Substrate stiffness modifies macrophages polarization in vivo subcutaneously

In order to investigate the effects of different stiffness on macrophages polarization in vivo, we implanted the polyacrylamide hydrogels with low, middle and high stiffness in 6-week-old male C57/BL6 mice subcutaneously for 14d. Cellular infiltration in the different groups was demonstrated by hematoxylin-eosin (H&E) staining (Fig. 6a). In the sham group, no cellular infiltration was found in the representative field. But in the hydrogel-implanted groups, cell infiltration happened subcutaneously. To investigate the phenotype of the infiltrated cells, we stained the tissue cells with anti-CD68 (in green), CD86 (in red) and CD206 (in red) fluorescent antibodies and analyzed the expression profiles of M1 and M2. Remarkably, the representative images (Fig. 6b–c) and the quantified data (Fig. 6d–e) showed that, compared to the infiltrated cells around the hydrogels with low substrate stiffness, less $CD68^+CD86^+$ cells and more $CD68^+CD206^+$ cells were significantly observed in the groups with middle and high substrate stiffness. It intuitively demonstrated that the low substrate stiffness hydrogels caused more macrophages to be polarized to M1 phenotype in *vivo*.

3.7. Substrate stiffness regulates nuclear factor kappa-B (NF-κB) signaling pathway in BMMs

We collected BMMs cultured on the hydrogels with different stiffness to study NIK activation, p65 phosphorylation and IκB kinase degradation in the cells by Western blot. As indicated in Fig. 7, compared with BMMs seeded on the TCP, the low substrate stiffness of the hydrogel promoted to activate NIK of BMMs, accelerated phosphorylation of p65 and IκB. However, with the gradually increased substrate stiffness stimulation for 24h, the expression of NIK in BMMs decreased significantly in sequence. In the same way, the ratio of phosphorylated p65 (pi-p65)/p65 and phosphorylated IκB (pi-IκB)/IκB also declined statistically. It is well-suggested the increased substrate stiffness enhanced the degradations of NIK. With the phosphorylation of p65 and IκB happened in the BMMs with the low substrate stiffness stimulation, NF-κB was set free and transported to the nucleus and caused downstream transcription of cytokines involved in the determination of BMMs polarization. Thus, low substrate stiffness stimulation was favorable of activating NF-κB signaling in BMMs and accelerate the production of pro-inflammation cytokines, such TNF-α and IL-1β which has already been reported [40].

4. Discussion

Cells receive mechanical information from the extracellular environment and then change the mechanical signals to biochemical signals through a process named mechanic-transduction, ultimately resulting in physiological responses and changes in gene expression [20]. During the past decades, cell matrix has attracted increasing attention in tissue healing and regeneration through facilitating cell differentiation or polarization toward a target lineage commitment. Such as, softer substrates stimulated an average 4 times IL-2 production and proliferation of human $CD4^+$ and $CD8^+$ T cells compared to stiffer substrates [41]. In recent years, the polarization of macrophages is of great significant since macrophage activation tends to be categorized into a series of functions. In the present study, we investigate the influence of extracellular matrix stiffness in microenvironment on the polarization of macrophages and the relevant mechanism.

The polyacrylamide hydrogels, as friendly biomaterials with gradient stiffness, were introduced to mimic ECM alternatives of different tissues, to study the effect of substrate stiffness on the polarization of macrophages. Specifically, three substrates were developed by add different concentration of acrylamide solution and bis-acrylamide solution. After the polyacrylamide hydrogels coagulated, their substrate stiffness was 2.55 ± 0.32 kPa (low, L), 34.88 ± 4.22 kPa (middle, M) and 63.53 ± 5.65 kPa (high, H), respectively. Their gradient stiffness is commensurate with the tissues of the collagen with Young's modulus (E) 0.1–4 kPa, the osteoid tissue with E ~25–40 kPa and the pre-calcified bone with E ~ 100 kPa, respectively [8,33,34]. Firstly, we aimed to study the biocompatibility of the polyacrylamide hydrogel with different substrate stiffness. In this study, we use Raw264.7 cells which can proliferate in vitro as the target cells, the results showed that whether the Raw264.7 cells were cultured in the supernatant or directly on the hydrogel, the growth curves showed no significant difference between the groups. After the BMMs were plated on the TCP or the

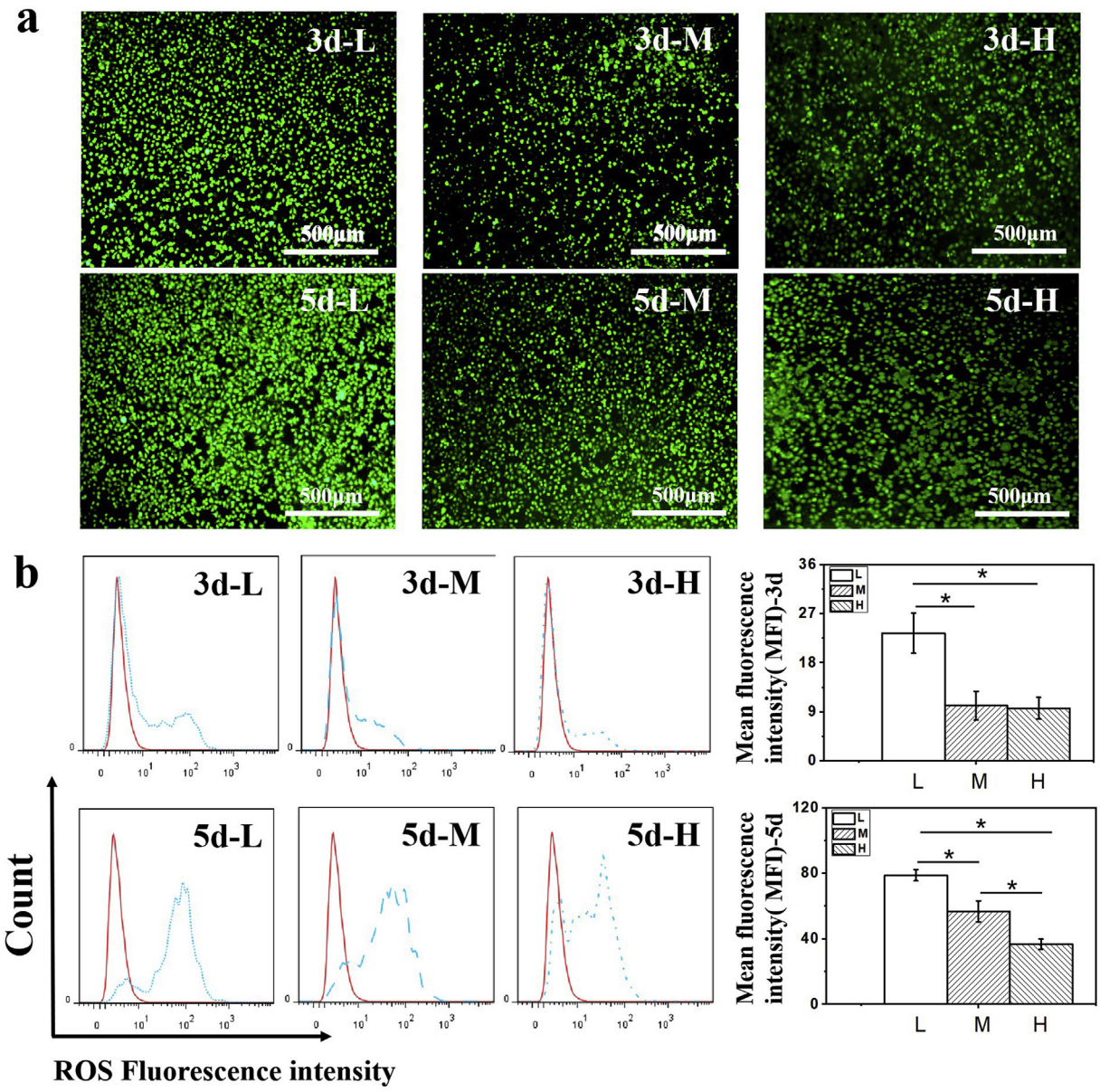

Fig. 5. Substrate stiffness controlled ROS production of BMMs. BMMs incubated on the polyacrylamide hydrogels with different substrate stiffness for 3d and 5d, respectively. (a) Images by the fluorescence microscope; (b) FCA analysis of ROS production; L: low substrate stiffness, M: middle substrate stiffness, H: high substrate stiffness, Solid red line: negative control, dash blue line: ROS, n = 3, $*p < 0.05$.

hydrogels for 5d, the data of live-dead cell staining showed no significant difference in dead cells between the groups. These data supported that hydrogels with different stiffness have a good biocompatibility. It also proved that substrate stiffness does not affect the proliferation of Raw264.7 cells.

Macrophages play an important regulatory role in different physiological and pathological processes. M1 release a variety of pro-inflammatory cytokines, immune activation factors, and chemokines, which therefore play an acute pro-inflammatory response, immune activation reactions, and phagocytosis [24]. In addition, it is well documented that at the late stage of injury, infiltrated monocytes are mainly polarized to M2 phenotype [38,42]. In addition to removing residual debris and down-regulating inflammation, M2 also secrete growth factors, such as TGF-β, VEGF, and EGF to promote fibroblast proliferation, support organization regeneration, maintain organizational function, and restore body homeostasis [43].

Based on the study of the effects of substrate stiffness on macrophage proliferation, we investigated the regulated effects of elastic models on the characteristics of macrophages. BMMs were cultured on the hydrogels for 3 and 5d respectively. Interestingly, BMMs appeared in the round shape seeded on the hydrogels with low and high modulus, while the cells became long and spindle-like on hydrogels with middle substrate stiffness, which was consistent with the reported study of Jan P. Stegemann et al. [38]. Pro-inflammatory M1 macrophages generally express IL-1β, IL-6, iNOS, and TNF-α with surface markers CD86. In contrast, anti-inflammatory M2 macrophages produce high levels of IL-4, ARG-1, TGF-β and IL-10 with surface markers CD163 and mannose receptor (CD206) [16]. Herein, we tested the characteristic indicators and the secretion of cytokines related to macrophages polarization. BMMs with low substrate stiffness expressed more CD86, IL-1β and iNOS and secreted more IL-1β and TNF-α in the supernatant than the cells with middle and high substrate stiffness. On the contrary, BMMs with middle and high substrate stiffness expressed more CD206 and Arg-1, secreted more IL-4 and TGF-β in the supernatant than the cells with low substrate stiffness. Therefore, substrate stiffness, did not affect the proliferation of macrophages, but obviously affect the polarization

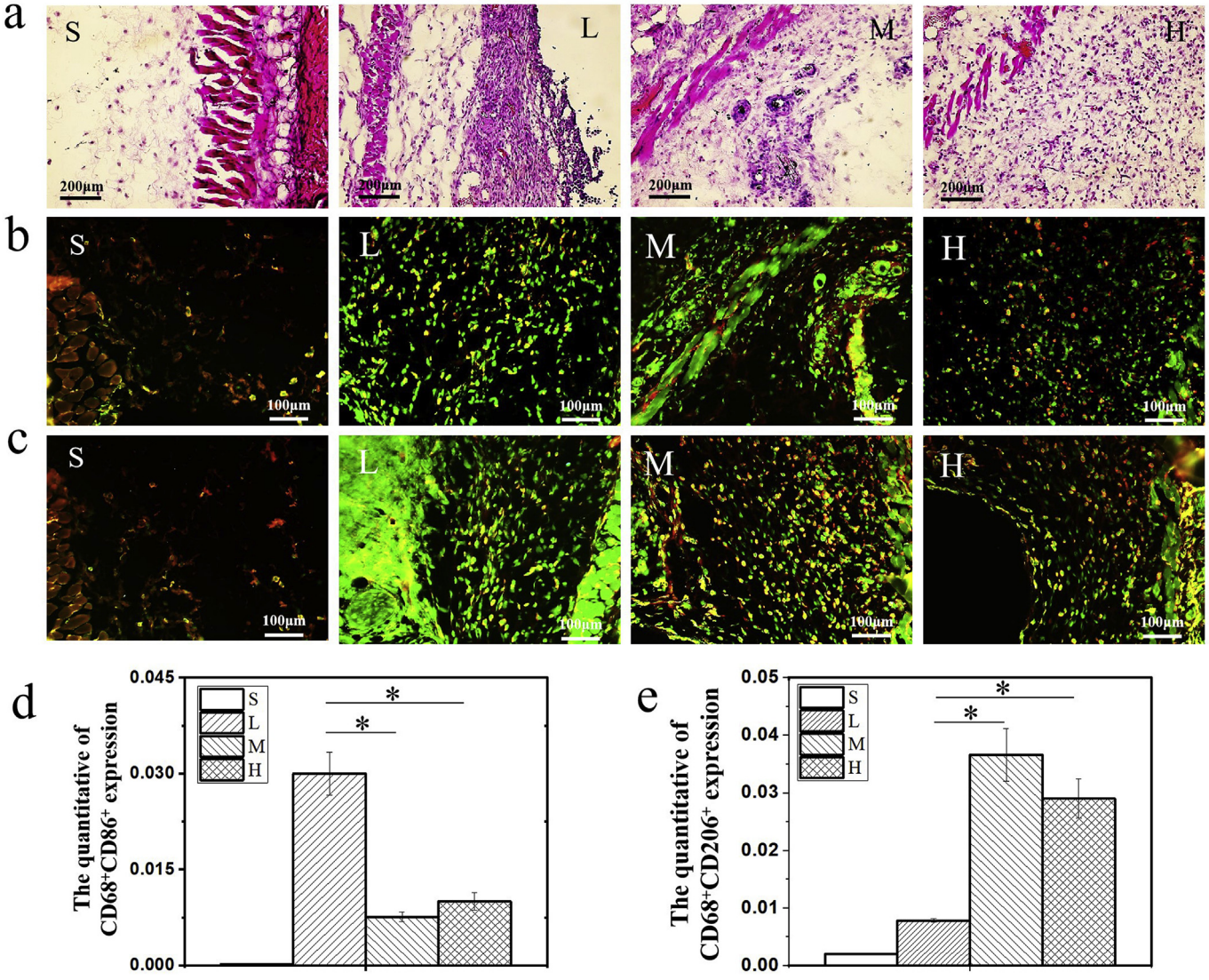

Fig. 6. Substrate stiffness monitored macrophage polarization in vivo. The polyacrylamide hydrogels were subcutaneously implanted into mice for 14d. (a) Representative slices with H&E staining; (b) and (c) Representative images with immunofluorescence staining of $CD68^+CD86^+$ and $CD68^+CD206^+$ subcutaneously; (d) and (e) Quantification analysis of $CD68^+CD86^+$ and $CD68^+CD206^+$ immunofluorescence density by Bioquant osteo; S: sham, L: low substrate stiffness, M: middle substrate stiffness, H: high substrate stiffness, n = 3, $^*p < 0.05$.

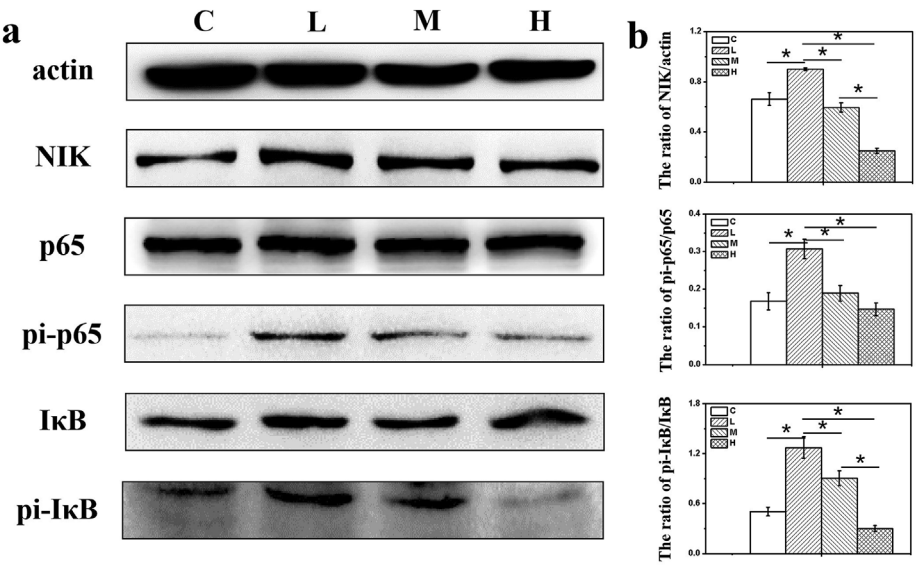

Fig. 7. Substrate stiffness affected NF-κB signaling pathway in BMMs. BMMs were cultured on the polyacrylamide hydrogels for 24h. (a) The representative expression of NIK, p65, pi-p65, IκB and pi-IκB in nuclear extracts of BMMs; (b) Quantitative analysis of the target proteins. C: TCP, L: low substrate stiffness, M: middle substrate stiffness, H: high substrate stiffness, n = 5, $^*p < 0.05$.

of macrophages.

Due to the more complicated microenvironment in vivo, modulation of macrophage phenotype represents a critical determinant of functional and the failure of implanted biomaterials [20]. We transplanted the polyacrylamide hydrogels with different stiffness under the skin of the mouse. After 14 days of implantation, the hydrogels and tissues were collected for morphological observation. Consistent with our in vitro results, more $CD68^+CD86^+$ cells surround the low substrate stiffness hydrogel, and more $CD68^+CD206^+$ macrophages surround the middle and high substrate stiffness hydrogel. Summarily, the substrate stiffness commensurate with the tissues of the collagen fibers, provide a favorable ECM stiffness to drive BMMs to M1; on the other hand, the substrate stiffness, commensurate with the tissues of the osteoid, contribute BMMs to M2 polarization.

Macrophage polarization is involved in many signaling pathways, such as NF-κB, JAK2/STAT3, ROS/ERK and mTOR signal pathway [44,45]. NF-κB pathway is critical to regulate many aspects of normal cellular functions as well as innate and adaptive immunity in response to pathogens and autoimmune stimuli [46]. Its activation is regulated by multiple levels of regulation, which can precisely adjust macrophage functions. Ferumoxytol nanoparticles suppress tumor growth by inducing M1 phenotype macrophage responses [22,47], the activation of NF-κB is one of the important factors that induce the differentiation of tumor associated macrophages into M1 [48]. By immunofluorescent staining and Western blot assay, we correspondingly observed that BMMs, stimulated with low substrate stiffness, expressed more ROS, NIK, phosphorylated-IκB and p65, and promote the activation of NF-κB signaling pathway. Our study further confirmed the previous research, which NF-κB p65 nuclear translocation is a marker of M1 macrophages [49].ROS have been reported as an upstream signaling to activate NF-κB p65 pathway [40]. Cucurbitacin E (CuE) could dampen the expression of pro-inflammatory cytokines in LPS-stimulated Raw264.7 cells, which was likely credited with the suppression of NF-κB nuclear *trans*-location [50]. We presumed that, the polyacrylamide hydrogels with low stiffness enhanced ROS production. The oxidative stress was linked to the activation of NF-κB p65 pathways, which give rise to the pro-inflammatory expression in BMMs [51].

In summary, the hydrogels with different stiffness have an effect on macrophage polarization. When solving different diseases, a suitable macrophage polarization for different diseases through the control of materials substrate stiffness are necessary. The results from this study provided a reasonable basis for the designing and selecting of appropriate substrates. On one hand, when designed for tumor therapy, macrophages should be polarized to M1 phenotype thus their matrix stiffness should be low. On the other hand, in the aspect of promoting tissue repair, we expect that macrophages can be polarized to the M2 phenotype, substrates with comparability to osteoid stiffness hydrogels are preferred to soft ones. Therefore, we expect that the substrate stiffness can modulate macrophage polarization to provide promising applications in the fields of tumor therapies and tissue repair.

So far, there are certain limitations to this study. We simply demonstrated that the polyacrylamide hydrogels with different substrate stiffness are able to regulate macrophage polarization, more biomaterials with different substrate stiffness need to be investigate. In addition, although our study concludes that hydrogels stiffness instructs macrophage polarization, simple mechanic-signaling and signaling pathway does not comprehensively explain the underlying cell behavior. Furthermore, the polarization of macrophages is unstable for high substrate stiffness hydrogels, which is probably the excessive stiffness of high substrate stiffness hydrogels cause this polarization instability.

In conclusion, our studies serve as a proof-of-concept that substrate stiffness modulate macrophages polarization through ROS-mediated NF-κB signaling pathway. We developed the polyacrylamide hydrogels with various stiffness, which have good biocompatibility. Macrophage polarization can be affected through sensing the stiffness of extracellular matrix. Collagen fibers stiffness-like substrate stiffness promotes M1 polarization, while an osteoid stiffness-like substrate stiffness contributes to M2 polarization. Accordingly, we anticipated substrate stiffness stimulation with immune modulation would facilitate the applications according to clinical needs, such as inflammation, tissue regeneration and anti-tumor.

CRediT authorship contribution statement

Mimi Chen: Conceptualization, Methodology, Writing - original draft. **Yu Zhang:** Conceptualization, Methodology, Writing - original draft. **Pinghui Zhou:** Methodology, Data curation. **Xingzhi Liu:** Data curation. **Huan Zhao:** Methodology, Data curation. **Xichao Zhou:** Methodology, Data curation. **Qiaoli Gu:** Methodology, Data curation. **Bin Li:** Conceptualization, Methodology, Data curation, Validation, Writing - review & editing. **Xuesong Zhu:** Conceptualization, Methodology, Data curation, Validation, Writing - review & editing. **Qin Shi:** Conceptualization, Methodology, Data curation, Validation, Writing - review & editing.

Declaration of competing interest

The authors declare that the research was conducted in the absence of any commercial or financial relationships that could be construed as a potential conflict of interest.

Acknowledgement

This work was supported by the National Natural Science Foundation of China (81772312, 891972059, 81772358), Research and Development of Biomedical Materials and Substitution of Tissue and Organ Repair under the National Key R&D Program (2016YFC1101502), the Natural Science Foundation of Jiangsu Province (BK2019668, BK20151210), Jiangsu Provincial Clinical Orthopedic Center, the Priority Academic Program Development of Jiangsu Higher Education Institutions (PAPD).

References

[1] K.C. Clause, T.H. Barker, Extracellular matrix signaling in morphogenesis and repair, Curr. Opin. Biotechnol. 24 (2013) 830–833, https://doi.org/10.1016/j.copbio.2013.04.011.
[2] I.T. Swinehart, S.F. B, Extracellular matrix bioscaffolds in tissue remodeling and morphogenesis, Dev. Dynam. 245 (2016) 351–360, https://doi.org/10.1002/dvdy.24379.
[3] A.D. Theocharis, S.S. Skandalis, C. Gialeli, N.K. Karamanos, Extracellular matrix structure, Adv. Drug Deliv. Rev. 1 (2015) 4–27, https://doi.org/10.1016/j.addr.2015.11.001.
[4] C.A. Lemarié, P.-L. Tharaux, S. Lehoux, Extracellular matrix alterations in hypertensive vascular remodeling, J. Mol. Cell. Cardiol. 48 (2010) 433–439, https://doi.org/10.1016/j.yjmcc.2009.09.018.
[5] R.O. Hynes, The extracellular matrix: not just pretty fibrils, Science 326 (2009) 1216–1219, https://doi.org/10.1126/science.1176009.
[6] J. Jang, H.J. Park, S.W. Kim, H. Kim, D.-W. Cho, 3D printed complex tissue construct using stem cell-laden decellularized extracellular matrix bioinks for cardiac repair, Biomaterials 112 (2016) 264–274, https://doi.org/10.1016/j.biomaterials.2016.10.026.
[7] J. Du, X. Chen, X. Liang, G. Zhang, C. Yang, Integrin activation and internalization on soft ECM as a mechanism of induction of stem cell differentiation by ECM elasticity, Proc. Natl. Acad. Sci. Unit. States Am. 108 (2011) 9466–9471, https://doi.org/10.1073/pnas.1106467108.
[8] A.J. Engler, S. Sen, H.L. Sweeney, D.E. Discher, Matrix elasticity directs stem cell lineage specification, Cell 126 (2006) 677–689, https://doi.org/10.1016/j.cell.2006.06.044 https://doiorg/101016/jcell200606044.
[9] P. Schedin, P.J. Keely, Mammary gland ECM remodeling, stiffness, and mechanosignaling in normal development and tumor progression, Cold Spring Harbor Perspect. Biol. 3 (2011) 3228–3238, https://doi.org/10.1101/cshperspect.a003228.
[10] M.V. Barbolina, Y. Liu, H. Gurler, M. Kim, A.A. Kajdacsy-Balla, L. Rooper, et al., Matrix rigidity activates Wnt signaling through down-regulation of dickkopf-1 protein, J. Biol. Chem. 288 (2013) 141–151, https://doi.org/10.1074/jbc.M112.431411.
[11] L.A. Matheson, G.N. Maksym, J.P. Santerre, R.S. L, Differential effects of uniaxial and biaxial strain on U937 macrophage-like cell morphology: influence of extracellular matrix type proteins, J. Biomed. Mater. Res. 81A (2010) 971–981, https://

doi.org/10.1002/jbm.a.31117.
[12] L. Huleihel, J.L.B.J. Dziki, T. Rausch, S.F. B, Macrophage phenotype in response to ECM bioscaffolds, Semin. Immunol. 29 (2017) 2–13, https://doi.org/10.1016/j.smim.2017.04.004.
[13] J. Du, Y. Zu, J. Li, S. Du, Y. Xu, L. Zhang, et al., Extracellular matrix stiffness dictates Wnt expression through integrin pathway, Sci. Rep. 6 (2016) 20395–20406, https://doi.org/10.1038/srep20395.
[14] S.J. Galli, N. Borregaard, T.A. Wynn, Phenotypic and functional plasticity of cells of innate immunity: macrophages, mast cells and neutrophils, Nat. Immunol. 12 (2012) 1035–1044, https://doi.org/10.1038/ni.2109.
[15] S.C. Funes, M. Rios, J. Escobar-Vera, A.M. Kalergis, Implications of macrophage polarization in autoimmunity, Immunology 154 (2018), https://doi.org/10.1111/imm.12910.
[16] B.N. Brown, B.D. Ratner, S.B. Goodman, S. Amar, S.F. Badylak, Macrophage polarization: an opportunity for improved outcomes in biomaterials and regenerative medicine, Biomaterials 33 (2012) 3792–3802, https://doi.org/10.1016/j.biomaterials.2012.02.034.
[17] L.B. Ivashkiv, Epigenetic regulation of macrophage polarization and function, Trends Immunol. 34 (2012) 216–223, https://doi.org/10.1016/j.it.2012.11.001.
[18] Siamon Gordon, Alternative activation of macrophages, Nat. Rev. 3 (2003) 23–35, https://doi.org/10.1038/nri978.
[19] A. Varin, S. Gordon, Alternative activation of macrophages: immune function and cellular biology, Immunobiology 214 (2009) 630–641, https://doi.org/10.1016/j.imbio.2008.11.009.
[20] F.Y. Mcwhorter, C.T. Davis, W.F.J.C. Liu, Physical and mechanical regulation of macrophage phenotype and function, Mole Life Sci Cmls 72 (2014) 1303, https://doi.org/10.1007/s00018-014-1796-8.
[21] Q. Gu, H. Yang, S. Q, Macrophages and bone inflammation. Journal of orthopaedic translation, J. Orthopaedic Translat. 10 (2017) 86–93, https://doi.org/10.1016/j.jot.2017.05.002.
[22] J. Choi, J. Gyamfi, H. Jang, J.S. K, The role of tumor-associated macrophage in breast cancer biology, Histol. Histopathol. 33 (2018) 133–145, https://doi.org/10.14670/HH-11-916.
[23] X. Wang, S. Chen, H. Ren, J. Chen, N. Huang, HMGN2 regulates non-tuberculous mycobacteria survival via modulation of M1 macrophage polarization, J. Cell Mol. Med. 23 (2019), https://doi.org/10.1111/jcmm.14599.
[24] J.C. Gensel, B. Zhang, Macrophage activation and its role in repair and pathology after spinal cord injury, Brain Res. 1619 (2015) 1–11, https://doi.org/10.1016/j.brainres.2014.12.045.
[25] J.E. Lim, E. Chung, Y. Son, A neuropeptide, Substance-P, directly induces tissue-repairing M2 like macrophages by activating the PI3K/Akt/mTOR pathway even in the presence of IFNγ, Sci Rep 7 (2017) 9417–9435, https://doi.org/10.1038/s41598-017-09639-7.
[26] J. Chang, C. Yang, C. Zhao, X. Wang, C. Wu, Stimulation of osteogenesis and angiogenesis by micro/nano hierarchical hydroxyapatite via macrophage immunomodulation, Nanoscale 11 (2019), https://doi.org/10.1039/C9NR05730G.
[27] Sherif Soliman, Shilpa Sant, Jason W. Nichol, Masoud Khabiry, Enrico Traversa, Khademhosseini, Controlling the porosity of fibrous scaffolds by modulating the fiber diameter and packing density, J. Biomed. Mater. Res. 96A (2011) 566–574 http://doi/org.10.1002/jbm.a.33010.
[28] M.L. Chamberlain, M.L. Godek, M. Gonzalez-Juarrero, D.W. G, Henotypic non-equivalence of murine (monocyte-) macrophage cells in biomaterial and inflammatory models, J. Biomed. Mater. Res. 21 (2009) 858–871, https://doi.org/10.1002/jbm.a.31930.
[29] X. Qiu, S. Liu, H. Zhang, B. Zhu, Y. Su, C. Zheng, Mesenchymal stem cells and extracellular matrix scaffold promote muscle regeneration by synergistically regulating macrophage polarization toward the M2 phenotype, Stem Cell Res. Ther. 9 (2018) 88–95, https://doi.org/10.1186/s13287-018-0821-5.
[30] E. Gibon, F. Loi, L.A. Córdova, J. Pajarinen, T. Lin, L. Lu, et al., Aging affects bone marrow macrophage polarization: relevance to bone healing, Regen Eng Transl Med 2 (2016) 98–104, https://doi.org/10.1007/s40883-016-0016-5.
[31] G.F. Vasse, P.T. Kühn, Q. Zhou, S.A. Bhusari, C. Reker-Smit, B.N. Melgert, et al., Collagen morphology influences macrophage shape and marker expression in?vitro, J Immunol Regenerative Med 1 (2018) 13–20, https://doi.org/10.1016/j.regen.2018.01.002.
[32] X.N. Zhao, Y.N. L, Y.T. W, Interleukin-4 regulates macrophage polarization via the MAPK signaling pathway to protect against atherosclerosis, Genet. Mol. Res. 15 (2016), https://doi.org/10.4238/gmr.15017348.
[33] A.L. Zajac, D.E. Discher, Cell Differentiation through Tissue Elasticity-Coupled, Myosin-Driven Remodeling vol. 20, (2008), pp. 609–615, https://doi.org/10.1016/j.ceb.2008.09.006.
[34] J.L. Leight, A.P. Drain, V.M. W, Extracellular matrix remodeling and stiffening modulate tumor phenotype and treatment response, Annu. Rev. Cell Biol. 1 (2017) 313–334, https://doi.org/10.1146/annurev-cancerbio-050216-034431.
[35] N. Mittal, F. Tasnim, C. Yue, Y. Qu, D. Phan, Y. Choudhury, et al., Substrate stiffness modulates the maturation of human pluripotent stem-cell-derived hepatocytes, Acs Biomater Sci 2 (2016) 1649–1657, https://doi.org/10.1021/acsbiomaterials.6b00475.
[36] Y. Gu, Y. Ji, Y. Zhao, Y. Liu, F. Ding, X. Gu, et al., The influence of substrate stiffness on the behavior and functions of Schwann cells in culture, Biomaterials 33 (2012) 6672–6681, https://doi.org/10.1016/j.biomaterials.2012.06.006.
[37] Małgorzata Witkowska-Zimny, Katarzyna Walenko, Anna Ewa Wałkiewicz, M. Lewandowska-Szumieł, Effect of substrate stiffness on differentiation of umbilical cord stem cells, Acta Biochim. Pol. 59 (2012) 261–264, https://doi.org/10.18388/abp.2012_2148.
[38] R.T. Annamalai, P.A.C.W. Turner, B. Levi, S. Kunkel, J.P. S, Harnessing macrophage-mediated degradation of gelatin microspheres for spatiotemporal control of BMP2 release, Biomaterials 16 (2018) 216–227, https://doi.org/10.1016/j.biomaterials.2018.01.040.
[39] A. Covarrubias, V. Byles, T. Homg, ROS sets the stage for macrophage differentiation, Cell Res. 23 (2013) 984–985, https://doi.org/10.1038/cr.2013.88.
[40] R.P. Nishanth, R.G. Jyotsna, J.J. Schlager, S.M. Hussain, P. Reddanna, Inflammatory responses of RAW 264.7 macrophages upon exposure to nanoparticles: role of ROS-NFκB signaling pathway, Nanotoxicology 5 (2011) 502–516, https://doi.org/10.3109/17435390.2010.541604.
[41] Roddy S. O'Connor, M. Xueli Hao, Keyue Shen, Keenan Bashour, Tatiana Akimova, C. Michael, M. Milone, Substrate rigidity regulates human T cell activation and proliferation %J journal of immunology, J. Immunol. 189 (2012) 1330–1339, https://doi.org/10.4049/jimmunol.1102757.
[42] Z. Peng, W. Gao, B. Yue, J. Jiang, Y. Gu, J. Dai, et al., Promotion of neurological recovery in rat spinal cord injury by mesenchymal stem cells loaded on nerve-guided collagen scaffold through increasing alternatively activated macrophage polarization, J Tissue Eng Regenerative Med 12 (2016) 1725–1736, https://doi.org/10.1002/term.2358.
[43] J.A. Shin, S.M. Lim, S.I. Jeong, J.L. Kang, E.-M. Park, Noggin improves ischemic brain tissue repair and promotes alternative activation of microglia in mice, Brain Behav. Immun. 40 (2014) 143–154, https://doi.org/10.1016/j.bbi.2014.03.013.
[44] T. Lei, L. Weiyang, Y. Le, C. Na, F. Xiaoting, J. Xiaofang, Cannabinoid receptor 1 participates in liver inflammation by promoting M1 macrophage polarization via RhoA/NF-κB p65 and ERK1/2 pathways, respectively, in mouse liver fibrogenesis, Front. Immunol. 8 (2017) 1214–1231, https://doi.org/10.3389/fimmu.2017.01214.
[45] Zong-Jian Liu, Yuan-Yuan Ran, Shu-Yan Qie, W.J. G, Melatonin protects against ischemic stroke by modulating microglia/macrophage polarization toward anti--inflammatory phenotype through STAT3 pathway, CNS Neurosci. Ther. 25 (2019) 1353–1362, https://doi.org/10.1111/cns.13261.
[46] M. Annemann, C. Plaza-Sirvent, M. Schuster, K. Katsoulis-Dimitriou, I. Schmitz, Atypical IκB proteins in immune cell differentiation and function, Immunol. Lett. 171 (2016) 26–35, https://doi.org/10.1016/j.imlet.2016.01.006.
[47] S. Zanganeh, G. Hutter, R. Spitler, Iron oxide nanoparticles inhibit tumour growth by inducing pro-inflammatory macrophage polarization in tumour tissues, CT224-CT224 http://doi.org/10.1038/nnano.2016.168, (2016) 74.
[48] U. Cho, B. Kim, S. Kim, Y. Han, Y.S. Song, Pro-inflammatory M1 Macrophage enhances metastatic potential of ovarian cancer cells through NF-κB activation, Mol. Carcinog. 57 (2017) 235–242, https://doi.org/10.1002/mc.22750.
[49] C. Porta, M. Rimoldi, G. Raes, L. Brys, P. Ghezzi, D.D. Liberto, et al., Tolerance and M2 (alternative) macrophage polarization are related processes orchestrated by p50 nuclear factor κB, Proc. Natl. Acad. Sci. Unit. States Am. 106 (2009) 14978–14983 https://doi.org/10.1073/pnas.0809784106.
[50] J. Qiao, X. Li-hui, H. Jian, O. Dong-yun, H. Xian-hui, The effects of cucurbitacin E on inflammatory responses of RAW264.7 macrophages induced by lipopolysaccharides and the underlying mechanism, Curr. Immunol. 4 (2012) 327–332.
[51] G.S. Youn, K.W. Lee, S.Y. Choi, J. Park, Overexpression of HDAC6 induces pro-inflammatory responses by regulating ROS-MAPK-NF-κB/AP-1 signaling pathways in macrophages, Free Radic. Biol. Med. 97 (2016) 14–23, https://doi.org/10.1016/j.freeradbiomed.2016.05.014.